

ORIGINAL MANUSCRIPT

Testosterone regulates thyroid cancer progression by modifying tumor suppressor genes and tumor immunity

Lisa J.Zhang, Yin Xiong, Naris Nilubol, Mei He, Swaroop Bommareddi, Xuguang Zhu¹, Li Jia², Zhen Xiao³, Jeong-Won Park¹, Xia Xu³, Dhaval Patel, Mark C.Willingham¹, Sheue-yann Cheng¹ and Electron Kebebew*

Endocrine Oncology Branch, ¹Laboratory of Molecular Biology and ²Bioinformatics Core Center for Cancer Research, National Cancer Institute, National Institutes of Health, Bethesda, MD 20814, USA and ³Laboratory of Proteomics and Analytical Technologies, Advanced Technology Program, Frederick National Laboratory for Cancer Research, Frederick, MD 21702, USA

*To whom correspondence should be addressed. Tel: +1 301 496 5049; Fax: +1 301 480 0599; Email: kebebew@mail.nih.gov

Abstract

Cancer gender disparity has been observed for a variety of human malignancies. Thyroid cancer is one such cancer with a higher incidence in women, but more aggressive disease in men. There is scant evidence on the role of sex hormones on cancer initiation/progression. Using a transgenic mouse model of follicular thyroid cancer (FTC), we found castration led to lower rates of cancer in females and less advanced cancer in males. Mechanistically, less advanced cancer in castrated males was due to increased expression of tumor suppressor (*Glipr1*, *Sfrp1*) and immune-regulatory genes and higher tumor infiltration with M1 macrophages and CD8 cells. Functional study showed that *GLIPR1* reduced cell growth and increased chemokine secretion (*Ccl5*) that activates immune cells. Our data demonstrate that testosterone regulates thyroid cancer progression by reducing tumor suppressor gene expression and tumor immunity.

Introduction

Cancer gender disparity in incidence, disease aggressiveness and prognosis has long been observed for a variety of human malignancies (1–3). Thyroid cancer, the most common cancer of the endocrine system, is one such cancer for which the incidence has dramatically increased over the last two decades (4). Thyroid cancer is 3–4 times more likely to develop in women, but it is more aggressive in men, who present with more advanced disease and have lower survival rates (5). Several hypotheses for the sex differences in thyroid cancer initiation and progression have been postulated, which include environmental and dietary factors, reproductive status, tumor sex hormone receptor expression status, body weight/body mass index and diabetes (2,6–8). However, there are limited experimental data demonstrating or establishing a mechanism by which sex differences in thyroid cancer initiation and progression may occur.

Although it has been postulated that sex hormones may account for cancer gender disparity, this has only been experimentally studied in hepatocellular carcinoma, where estrogen was found to inhibit interleukin-6 secretion and thus decrease and prevent chemically induced liver carcinogenesis in mice (9–11). In thyroid cancer, *in vitro* evaluation of the effects of sex hormones on cultured cells and the analysis of androgen receptor status in tumor tissues have yielded conflicting results (2). To understand the molecular mechanism of thyroid cancer sex differences, an *in vivo* model that recapitulates the sex differences in thyroid cancer initiation and progression would be required.

Understanding the role of sex hormones on cancer initiation and progression would provide a better understanding of the biological basis for cancer gender disparity and could have implications for cancer therapy and prognostication. We

Abbreviations

FTC	follicular thyroid cancer
siRNA	small interfering RNA
TSH	thyroid-stimulating hormone

evaluated the effect of sex hormones on thyroid cancer initiation and progression using *Thrb^{PV/PV}* transgenic mice, a model that mimics human follicular thyroid cancer (FTC) development. Like human FTC, the mouse tumors have capsular and vascular invasion and develop metastases (12). We found that in *Thrb^{PV/PV}* mice, castration of female mice was associated with a lower rate of thyroid cancer, and castration in male mice was associated with less advanced thyroid cancer. Our follow-up studies in the male mice suggested a testosterone-regulated cross talk between tumor suppressor genes (*Glpr1* and *Sfrp1*) and tumor-specific inflammation, which could play a role in modulating cancer progression. We validated the disease aggressiveness observed in our mouse model in human FTC by analyzing population-based cancer registry data. Lastly, our functional studies show that *GLIPR1* has tumor suppressive effects and modulates *Ccl5* secretion, a chemokine known to have a role in recruitment and activation of immune cells (13).

Materials and methods

Mice

Thrb^{PV/PV} mice and their wild-type control littermates were generated and genotyped as described previously (14). The National Cancer Institute Animal Care and Use Committee approved the animal protocol.

Hormone pellet

Continuous-release testosterone pellets (12.5 mg/pellet, 60-day release or 18.75 mg/pellet, 90-day release) that release testosterone at 0.21 mg/day or placebo pellets were purchased from Innovative Research of America (Sarasota, FL).

Surgical procedures

Orchiectomy/oophorectomy or sham surgeries were performed on 6-week-old mice. Sham surgeries were performed by visualizing the ovary/testicle and replacing it back into the abdomen prior to closure. Testosterone or placebo pellet was placed in a subcutaneous pocket, and pellet reimplants were performed every 2–3 months, depending on the pellet used, until the mice reached 8–9 months of age. The mice were then euthanized, and their blood, thyroids and other organs were collected. At the time of collection, half of the tissue samples were frozen in liquid nitrogen and the other half were fixed immediately in neutralized 10% formalin. Body and thyroid weights were measured at necropsy.

Quantitation of serum hormones

Mouse blood was harvested at necropsy and serum was collected. Serum sex hormones and thyroid-stimulating hormone (TSH) analysis was carried out as described previously (15).

Histology, immunohistochemistry and immunofluorescence staining

Tissues were fixed in 10% formalin, embedded in paraffin, and hematoxylin and eosin-stained slides were evaluated by a pathologist. For immunohistochemistry, sections were incubated with primary antibody (rabbit anti-CD68, Abcam, or rat anti-mouse CD8 α , LSBio) at 4°C overnight, and immunostaining was performed using Vectastain ABC and DAB kits (Vector Laboratories, Burlingame, CA). Primary antiserum was omitted in the negative control. For immunofluorescence staining, sections were incubated with primary antibodies, fluorescein isothiocyanate-labeled rat anti-F4/80 (Abcam) and rabbit anti-inducible nitric oxide synthase 2 (iNOS) (LSBio) at 4°C overnight, and then stained with Alexa Fluor® 594 goat anti-rabbit IgG (H+L) antibody.

RNA isolation and quantitative real-time reverse transcription-PCR

Total RNA was extracted using TRIzol reagent (Invitrogen) and reverse transcribed with a high-capacity complementary DNA reverse transcription kit (Applied Biosystems). The relative messenger RNA amounts were determined using TaqMan gene expression assays (Applied Biosystems) on an ABI 7900 HT system; β -glucuronidase was used as an endogenous control.

Genome-wide messenger RNA expression microarray

Total RNA was used for complementary DNA reverse transcription, synthesis, amplification, fragmentation and terminal labeling with GeneChip WT Sense Target Labeling and Control Reagents (Affymetrix, Santa Clara, CA). Complementary DNA was hybridized to Affymetrix Mouse Gene 1.0 ST Array GeneChip. The arrays were washed and stained using the fluidics protocol FS450_0007 procedure on an Affymetrix Fluidics Station 450. The probe intensities were scanned by GeneChip Scanner 3000.

The raw data were normalized and analyzed using the Partek Genomic Suite (Partek, St Louis, MO). Analysis of variance was used, and the gene list was generated that have significant differential expression at false discovery rate (FDR) ≤ 0.05 and 1.3-fold or more differences. Pathway analysis was performed using the ingenuity pathway analysis bioinformatics resources (Redwood City, CA).

Small interfering RNA transfection

FTC-133 and HEK-293 cells were used. FTC cell line FTC-133 was kindly provided by Dr Peter Goretzki, Neuss, Germany, and was authenticated by short-tandem repeat profiling on 14 October 2012; HEK-293 was purchased from ATCC at 11 October 2012.

The small interfering RNA (siRNA) for human *GLIPR1* (siRNA ID: s21675) and scrambled negative control (Part#: 4390844) were purchased from Applied Biosystems. FTC-133 and HEK-293 cells were reverse transfected with each individual siRNA at a concentration of 80 nmol/l using Lipofectamine RNAiMAX (Invitrogen). Total RNA was isolated and the level of *GLIPR1* messenger RNA was determined by quantitative reverse transcription-PCR.

Cell proliferation and clonogenic assays

For cell proliferation, cells were reverse transfected with individual siRNA in 96-well black plates at 1.2×10^3 cells per well for FTC-133, or 2.5×10^3 cells per well for HEK-293, and maintained in a humidified incubator. CyQuant proliferation assays were performed according to manufacturer's instructions (Invitrogen).

To perform clonogenic assay, cells transfected with individual siRNA were trypsinized, and 600 cells were seeded into each well of six-well plates that had been coated with 0.1% gelatin. Cells were cultured in a humidified incubator for 2 weeks. The colonies were fixed with 4% paraformaldehyde and stained with crystal violet (0.05% wt/vol).

Cytokine array

FTC-133 cells were transfected with individual siRNA, and the culture media was changed 2 days after transfection. Then the cells were kept in the same media for up to 5 days after transfection. The culture media was collected and centrifuged at 4500 r.p.m. for 20 min. The supernatants were used to detect the released cytokines using Human cytokine array panel A from R&D systems.

Surveillance, Epidemiology and End Results data acquisition and analysis of human FTC

Clinical data from 1988 to 2007 of all adult patients (≥ 20 years of age) with a diagnosis of FTC (8330–8332) were captured from National Cancer Institute's Surveillance, Epidemiology and End Results Program. Follicular variants of papillary thyroid cancer were excluded. All patients had thyroid cancer as the first and only primary cancer. Clinical characteristics and outcome were compared by sex.

Statistical analysis

Pearson's chi-square test was used to assess the differences among groups for nominal categorical variables. The Mann–Whitney test was used to compare non-parametric variables and unpaired t-test for parametric

variables. A two-tailed P-value of <0.05 was considered statistically significant. Statistical analysis was performed using SPSS® v16.0 for Windows (SPSS, Chicago, IL) and GraphPad Prism 5.

Sex hormone receptor binding site analysis

The sex hormone receptor binding site analysis was performed by using MatInspector Release professional 8.06, August 2012; database version EIDorado 08-2011 and MatInspector library Matrix Family Library Version 8.4 (June 2011).

Results

Effect of sex hormones on thyroid cancer initiation and progression in *Thrb^{PV/PV}* mice

Thrb^{PV/PV} mice spontaneously develop FTC in a pattern similar to humans (12), we thus tested the idea that these mice could be used as a model system to study the effect of sex hormones on thyroid cancer initiation and progression. The rate and extent of thyroid cancer in 23 *Thrb^{PV/PV}* mice, 5–14 months old, were evaluated by sex. Both male and female mice developed thyroid cancer with histopathology showing capsular invasion, vascular invasion and anaplasia. There was a significantly higher rate of distant metastasis in male mice compared with female (45% versus 17%, $P < 0.05$), with 7 of 23 *Thrb^{PV/PV}* mice developing distant metastases (7 with lung metastases, 2 also had heart metastases).

To determine the effect of sex hormones on thyroid cancer initiation and progression, we performed sham surgery or castration (orchietomies in males and oophorectomies in females) on 6-week-old *Thrb^{PV/PV}* mice and examined the histopathologic features of the mouse thyroid when the mice reached 8–9 months old. In females, we found a higher rate of thyroid cancer in sham-oophorectomized females than in oophorectomized female mice (Figure 1A). In male mice, we found significantly larger tumors in sham-orchietomized male mice than those who had orchietomies (Figure 1B and C). No difference in lung metastasis was seen between castration and sham groups in both male and female mice. Successful ablation of sex hormone production in the mice that had orchietomies or oophorectomies was confirmed by measuring serum testosterone and progesterone, as well as 15 sex hormone metabolites (Supplementary Figure S1, available at Carcinogenesis Online). Also, to exclude the possibility that the surgical procedures may have influenced TSH levels, which are high in this transgenic mouse model of FTC and are required to induce metastatic FTC in *Thrb^{PV/PV}* mice, we also measured mouse serum TSH and found similar TSH levels among the four different experimental groups (Supplementary Figure S2, available at Carcinogenesis

Online). These results suggest that in *Thrb^{PV/PV}* mice, female sex hormones influence thyroid cancer initiation, whereas male sex hormones promote thyroid cancer progression.

Effect of testosterone on thyroid cancer gene expression profile

Because we observed a striking difference in tumor size between the male mice with or without castration, we focused our follow-up studies on determining the mechanism by which male sex hormones (testosterone) could regulate thyroid cancer progression. To explore this, we performed genome-wide gene expression analysis on the thyroid cancer samples from the sham-surgery male and orchietomized male mice and found distinctly different gene expression profiles between the two groups, which showed a complete separation by sex hormone status (Figure 2A). Pathway analysis of the differentially expressed genes showed genes involved in immunity were significantly overrepresented (Supplementary Table S1, available at Carcinogenesis Online).

If these differentially expressed genes were directly related to male sex hormone, we reasoned that similar changes should also be observed when comparing thyroid cancer samples from the sham-surgery male mice to those from the oophorectomized female mice who also had no sex hormone(s). Indeed, comparable differentially expressed genes and pathways were revealed by the gene expression profile comparison of cancer samples between sham-surgery males and oophorectomized female mice (Figure 2B and C; Supplementary Tables S1–S4, available at Carcinogenesis Online). Furthermore, most of the top differentially expressed genes between the sham-surgery male mice and the castrated male or female mice contain testosterone receptor binding sites (Figure 2C). This suggests that the differences in gene expression profiles and pathways identified in the thyroid cancer samples were specific to the sex hormone status of the mice.

If the difference in thyroid cancer progression was due to sex hormones, we next postulated that removing sex organs in mice should eliminate this difference. Indeed, no difference was observed by comparing thyroid cancer tumor size/weight from the castrated male and female mice (Figure 2D). Even more striking, the gene expression profile comparison of the thyroid cancer samples from these mice revealed that only two genes were differentially expressed (with <1.5-fold difference) excluding X- or Y-linked genes (Figure 2E). These data further supported our hypothesis that the observed cancer sample gene expression differences between sham-surgery male mice versus castrated male or female mice were directly due to endogenous male sex hormone (testosterone), thus suggesting that testosterone plays a role in thyroid cancer progression in *Thrb^{PV/PV}* mice.

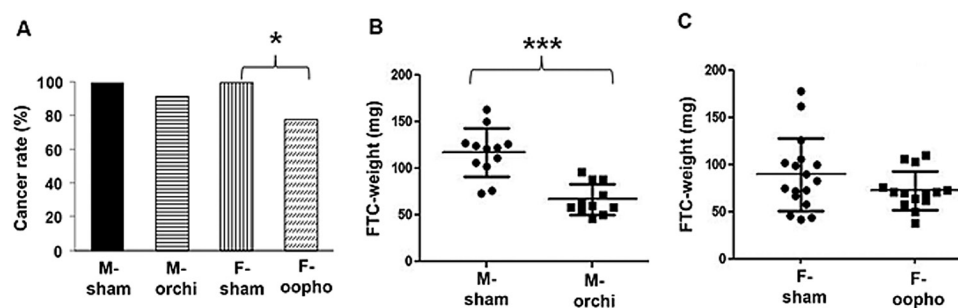


Figure 1. Thyroid cancer initiation and progression by sex hormone status. (A) Thyroid cancer rates in each group by sex and castration status. (B) Thyroid tumor size (measured by weight) from orchietomized and sham-orchietomized male mice. (C) Comparisons of thyroid tumor size in oophorectomized and sham-oophorectomized female mice. Error bars are \pm SEM. * $P < 0.05$, *** $P < 0.001$. orchi = orchietomy, oopho = oophorectomy.

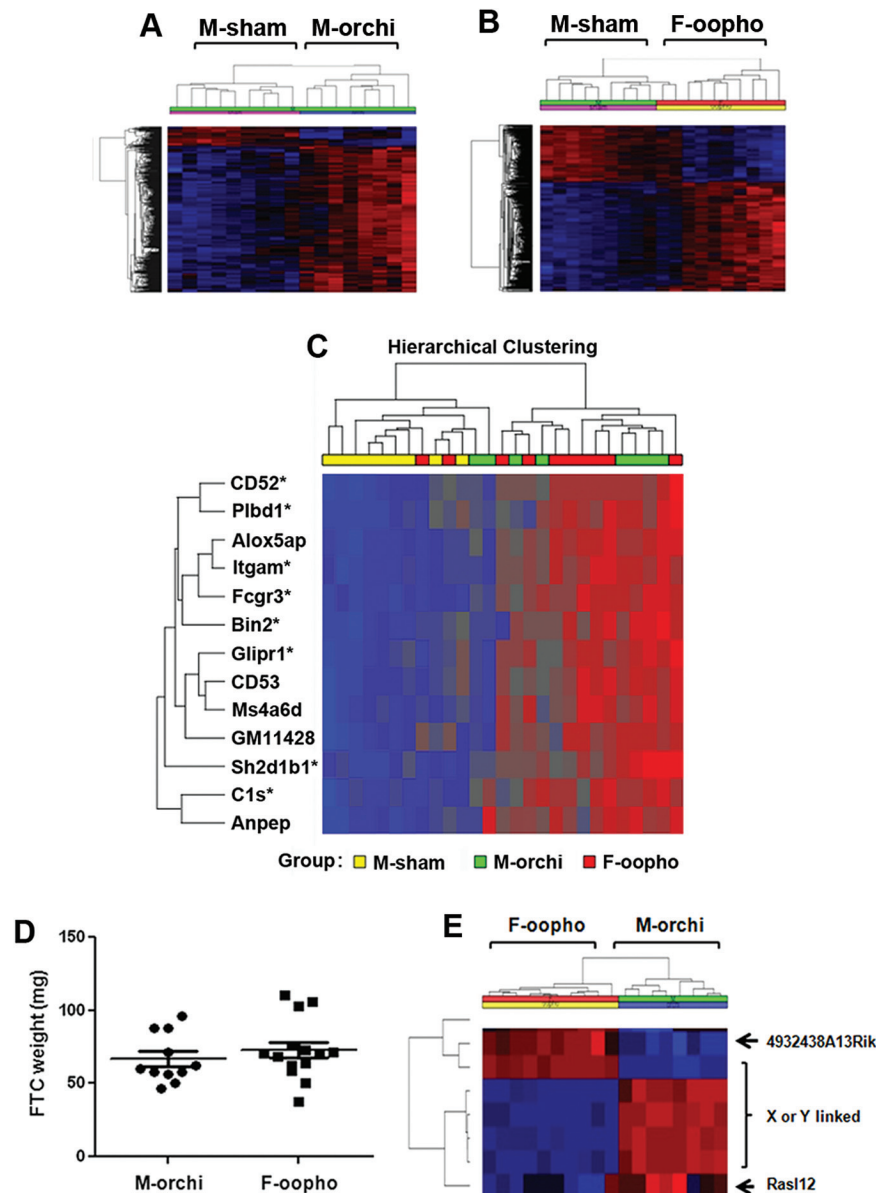


Figure 2. Genome-wide gene expression profiles of thyroid cancer samples. (A) Unsupervised hierarchical cluster analysis of top variably expressed genes (FDR < 0.05) between M-sham and M-orchietomized mice. Each row represents the expression level of an individual gene and each column represents an individual tumor sample. Overexpressed genes are indicated in red and underexpressed genes are indicated in blue. (B) Unsupervised hierarchical cluster analysis of top variably expressed genes (FDR < 0.05) between M-sham and F-oophorectomized mice. (C) Hierarchical cluster analysis of top differentially expressed genes between sham-surgery males and orchietomized males or oophorectomized females (FDR < 0.05, fold-change > 1.7). *Indicates gene that contains a testosterone receptor binding site(s). (D) Comparisons of thyroid tumor sizes in castrated male and female mice. Error bars are \pm SEM. (E) Unsupervised hierarchical cluster analysis of top variably expressed genes in castrated male and female mice (FDR < 0.05). orchi = orchietomy, oopho = oophorectomy.

Testosterone regulates tumor suppressor gene expression and modulates thyroid cancer immune cell infiltration

As mentioned above, our microarray analysis identified several differentially expressed genes in thyroid cancer samples isolated from sham-surgery male mice versus castrated male mice (Supplementary Tables S3 and S4, available at *Carcinogenesis* Online). Thus, we validated the expression differences of these genes by quantitative reverse transcription-PCR. Compared with orchietomized males, the thyroid cancer samples from the sham-castrated male mice had lower expression of *CD52*, *Sh2d1b1*, *Fcgr3*, *Itgam*, *Glipr1* and *Sfrp1*, all of which have

testosterone receptor binding site(s) (Supplementary Figure S3, available at *Carcinogenesis* Online).

Given the differential expression of *CD52*, *Sh2d1b1*, *Fcgr3* and *Itgam*, all expressed in immune cells, we next asked whether there were any inflammatory cells in the thyroid cancers samples and whether the differentially expressed immune-regulatory genes were specific to FTC cells or present in the tumor stroma or in infiltrating macrophages and lymphocytes. To determine this, we evaluated the expression of *CD68* and *CD8 α* by immunohistochemistry. We found strong *CD68* staining, a phagocytic marker, in thyroid tumor tissues, where it was restricted to tumor infiltrating macrophages (Figure 3A). Furthermore, the castrated male mice with smaller thyroid

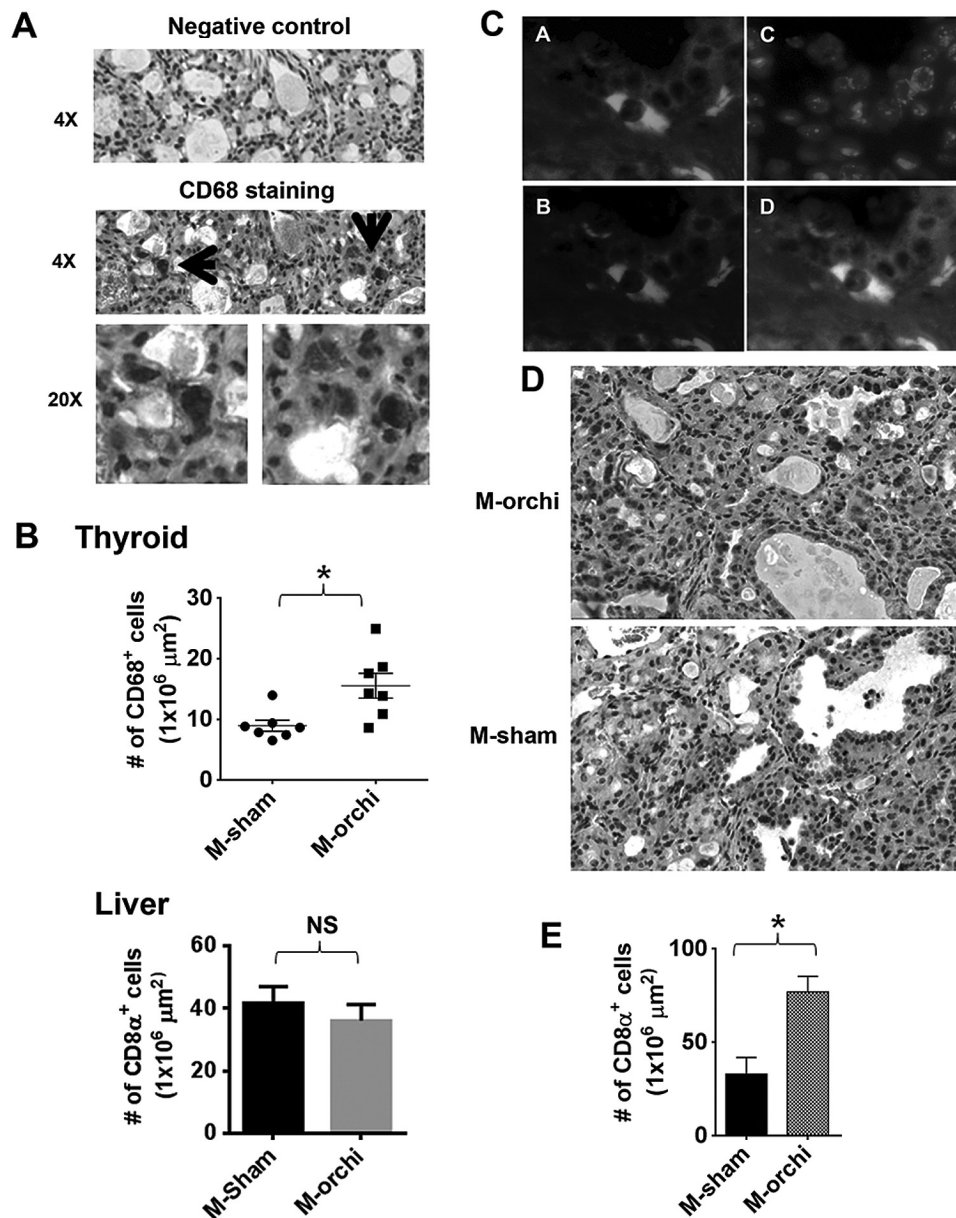


Figure 3. Castration of male mice increases CD68- and CD8α-positive cells in FTC. (A) Immunostaining of CD68-positive macrophages. (B) Macrophage density comparison between castrated and sham-castrated males. Upper panel: macrophage densities in thyroid cancer samples. Lower panel: macrophage densities in liver samples. Mean macrophage densities \pm SEM of seven random areas of representative liver samples. Error bars are \pm SEM. * $P < 0.05$. (C) Representative immunofluorescence staining images of F4/80 (A), INOS (B), 4',6'-diamidino-2-phenylindole (C) and merged image (D). (D) Representative images of CD8α immunostaining. (E) Thyroid cancer CD8α-positive cell densities of castrated and sham-castrated males. Error bars are \pm SEM. * $P < 0.05$. orchi = orchietomy, oopho = oophorectomy.

tumors had a higher density of CD68-positive cells in their tumors than those of sham-surgery group (Figure 3B). We did not see difference in CD68-positive cells in the liver suggesting that the observed difference was specific to thyroid cancer (Figure 3B). To distinguish between M1 and M2 macrophages in the thyroid cancer samples, we performed coimmunofluorescent staining with F4/80 and INOS, markers specific for M1 macrophages (16), and found that most F4/80-positive cells were also positive for INOS, suggesting that they were M1 macrophages (Figure 3C). Furthermore, the numbers of CD8α-positive cells were also higher in the thyroid cancers of castrated males when compared with that of sham-surgery males (Figure 3D,E). These results suggested that male sex hormones suppress thyroid cancer immunity.

Testosterone promotes thyroid cancer progression

To confirm the effect of male sex hormone on thyroid cancer progression, we performed sham surgery or castration on 6-week-old male mice and replaced testosterone in a group of castrated mice using subcutaneous pellet implants that continuously released testosterone. The mice were maintained until 8–9 months old, and then we examined their serum testosterone level and thyroid tumor status. As shown in Figure 4A, testosterone implantation reconstituted the testosterone level in the castrated mice to the similar level found in the sham-castrated mice. More importantly, testosterone implantation after castration resulted in significantly larger thyroid tumors (Figure 4B).

To test whether testosterone promotes thyroid cancer progression through suppressing tumor immunity and changing

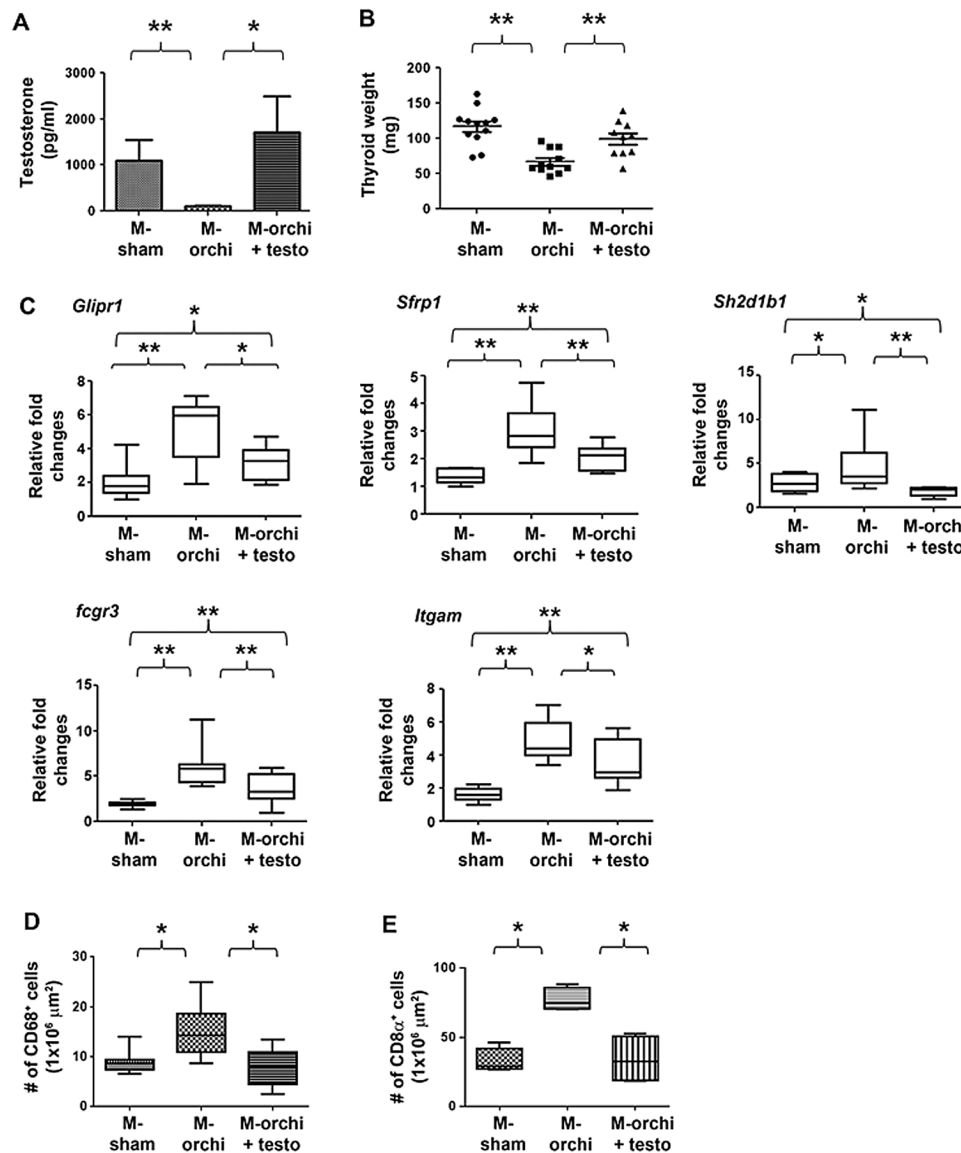


Figure 4. Testosterone promotes thyroid cancer progression. (A) Mouse serum testosterone concentrations at necropsy. (B) Comparisons of mouse thyroid cancer sizes. (C) Quantitative reverse transcription-PCR detection of differentially expressed genes. (D) Macrophage densities in thyroid cancer in different groups. (E) CD8 α -positive cell densities in thyroid cancer samples in the different groups. Box plot is for median with 5th and 95th percentiles. * $P < 0.05$; ** $P < 0.01$.

tumor gene expression profile, we determined the gene expression profile and the density of CD68- and CD8 α -positive cells in the tumors from the different groups of mice. We found that reconstitution of testosterone in the castrated males reversed the gene expression profile to that of the sham-castrated males and resulted in a lower number of CD68- and CD8 α -positive cells in their tumors (Figure 4C–E).

Gender disparity in human FTC

Given our experimental data showing higher rates of FTC in sham-oophorectomized female mice and more aggressive tumors in sham-orchietomized male mice, we wanted to determine if this mouse model was representative of human FTC. Thus, data of all adult patients (≥ 20 years of age) from 1988 to 2007 with a diagnosis of FTC were analyzed using the National Cancer Institute's Surveillance, Epidemiology and End Results Program database. We found a significantly higher rate

of FTC in reproductive-age women (Supplementary Figure S4A, available at *Carcinogenesis* Online); the female-to-male ratio was 4.1:1 in patients <45 years old. When comparing the rate of larger primary or locally advanced tumors by sex, men had higher rates than women (Supplementary Figure S4B, available at *Carcinogenesis* Online). Furthermore, there was higher FTC-associated mortality in men than women in the 40- to 60-year age group (Supplementary Figure S4C, available at *Carcinogenesis* Online). These data are consistent with our experimental data that showed sex differences in FTC initiation and progression in *Thrb^{PV/PV}* mice by sex and sex hormone status and suggest that this mouse model is relevant to human FTC.

GLIPR1 has a tumor suppressive effect and modulates the secretion of Ccl5

GLIPR1 has been implicated to have tumor suppressor function in prostate cancer (17) but has not been studied in thyroid

cancer. Thus, we studied the function of *GLIPR1* using a human FTC cell line (FTC-133) and the HEK-293 cell line, which had basal expression of *GLIPR1*. We found that knockdown of *GLIPR1* increased cellular proliferation and colony formation in vitro (Figure 5A and B; Supplementary Figure S5, available at Carcinogenesis Online). Given that we observed the reduced tumor immunity in sham-castrated male mice whose tumor also had lower expression of *Glipr1*, and it has been reported previously that intra-tumoral administration of *Glipr1* increases the tumor-associated immune cells infiltration in prostate cancer (18), we asked whether *GLIPR1* regulates chemokine expression in cancer cells that could mediate a tumor immune response. We performed chemokine profiling of 36 key cytokines implicated in tumor immunity and cancer biology using cell culture supernatants with and without *GLIPR1* knockdown (Supplementary Table S5, available at Carcinogenesis Online). We found that *GLIPR1* knockdown reduced *Ccl5* secretion, a chemokine that has a strong chemotactic activity toward multiple immune cells, such as monocytes and cytotoxic T lymphocytes (Figure 5C). We also found higher *Ccl5* expression levels in tumor samples from the orchietomized male mice as compared with those from sham-orchietomized and orchietomized males with testosterone implantation (Figure 5D). These findings taken together suggest that reduced *GLIPR1* expression can promote cellular growth and a chemokine profile that facilitates reduced tumor immunity.

Discussion

To our knowledge, this is the first study to determine if sex hormones influence thyroid cancer initiation and progression in a transgenic mouse model, with validation of the observed differences using a population-based cancer registry data that recapitulate the observed difference in FTC by sex. In *Thrb^{PV/PV}* mice that had no alteration in sex hormone levels, the male mice developed more aggressive FTC, which is consistent with the development of more aggressive FTC in men. When sex hormones were ablated in *Thrb^{PV/PV}* mice, the castrated female mice developed lower rates of FTC than the sham-surgery female mice, and the castrated males had smaller tumors than the sham-surgery male mice.

Given the observed differences of thyroid cancer progression in *Thrb^{PV/PV}* mice based on testosterone status, we performed genomic studies to better understand the molecular basis for these differences. We demonstrated that the tumors from castrated and sham-castrated mice possess distinct gene expression profiles. The principle gene signatures associated with this difference were *Glipr1*, *Sfrp1* and immune-regulatory genes, many of which have testosterone response elements. Moreover, we showed that the differential expression of the immune-regulatory genes was associated with different levels of infiltrating immune cells such as M1 macrophage and CD8 α -positive cells in the cancer samples.

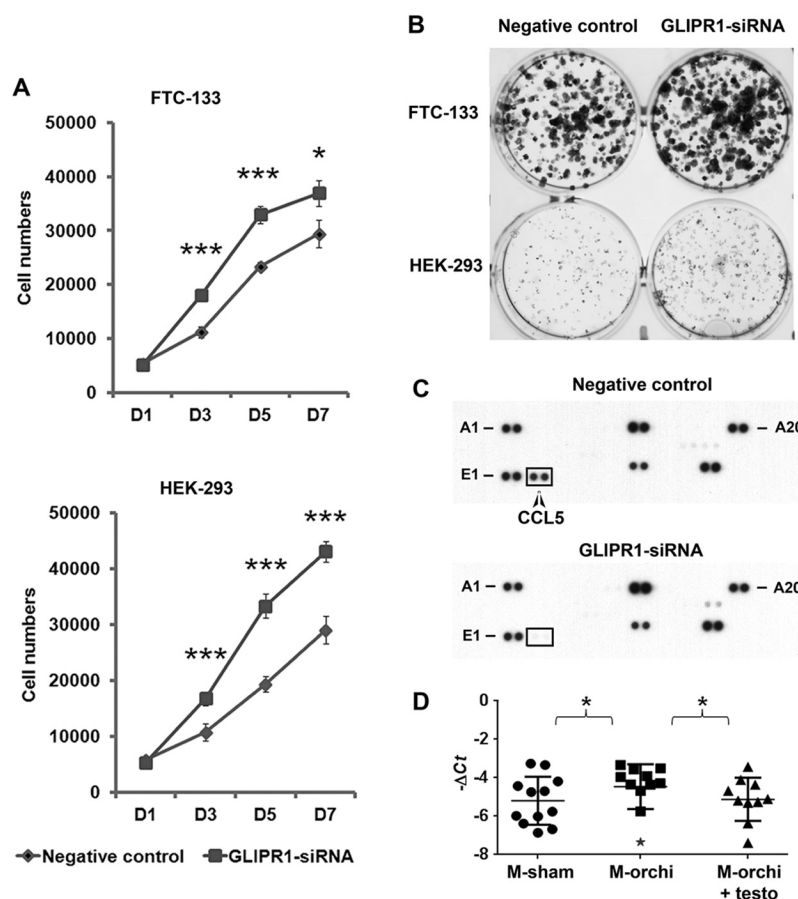


Figure 5. *GLIPR1* knockdown increases cell proliferation and colony formation and reduces the release of *Ccl5*. FTC-133 and HEK-293 cells were transfected with negative control siRNA or *GLIPR1* siRNA. Then cell proliferations (A) and colony formation (B) were examined. (C) Detection of released cytokines, chemokines and acute phase proteins from the culture media of FTC-133 cells transfected with the indicated siRNA. (D) *Ccl5* expression in mouse thyroid cancer samples by quantitative reverse transcription-PCR. Significant outlier identified by QuickCalcs (GraphPad) is indicated by asterisk. **P* < 0.05 (calculated by excluding outlier).

GLIPR1 is a secreted and membrane-bound protein. It contains p53-binding elements and is upregulated by p53 and has a growth suppressive effect (19). GLIPR1 also shows anti-angiogenic, immunostimulatory and metastasis-suppressing activities. In prostate cancer, GLIPR1 upregulation increases the production of reactive oxygen species, leading to p53-independent activation of the c-Jun N-terminal kinase/c-Jun pathway and the inhibition of anti-apoptotic molecule Bcl2. GLIPR1 upregulation also decreases β -catenin signaling that leads to decreased expression of MYC and increased p21 expression and results in cell cycle arrest (17,20). In an orthotopic mouse prostate cancer model, intra-tumoral administration of adenoviral vector-mediated *Glipr1* expression reduces primary tumor size and lung metastasis and increases the infiltration of tumor-associated macrophages, dendritic cells and CD8-positive T cells (18). The intra-prostatic administration of GLIPR1 expressed by an adenoviral vector in men has also been observed to have some antitumor activity and results in increased immune response (21). It has been reported recently that a recombinant, truncated form of GLIPR1 (GLIPR1- Δ TM) induces apoptosis and mitotic catastrophe in prostate cancer cells and suppresses tumor growth after systemic injection (22,23). Ccl5 is a chemokine and plays an important role in chemotaxis and activation of a wide spectrum of immune cells. It has a strong chemotactic activity toward monocytes and cytotoxic T lymphocytes (13). Our findings that in the FTC of sham-orchietomy mice, there is reduced expression of *Glipr1* and reduced M1 macrophages and CD8-positive T cells as compared with FTC samples from the orchietomy group with smaller tumors suggest an immune-mediated difference in thyroid cancer progression in the mouse model. This is further supported by our finding that GLIPR1 had tumor suppressive effects in addition to the effect on Ccl5 secretion observed *in vitro*.

The immune system has a dual function in cancer: inflammation leading to cancer initiation and progression and also showing tumor suppressive and specific immunity (24). In thyroid cancer, this duality of the immune system is remarkable. Chronic lymphocytic thyroiditis is a common autoimmune disorder with a female preponderance. Several investigators have suggested an association between thyroid cancer in individuals with chronic lymphocytic thyroiditis, which is consistent with the link established between inflammation and cancer initiation and progression (25,26). On the other hand, several investigators have shown a protective role of lymphocytic thyroiditis, with less aggressive disease and better patient outcome reported in those with thyroid cancer and coexisting thyroiditis (27). Also, several studies have shown the existence of a tumor-specific immune response with tumor-associated lymphocytic infiltrates and macrophages (28). In the current study, we found that testosterone promoted thyroid cancer progression, suppressed the expression of multiple immune-regulatory genes and reduced the infiltration of CD68- and CD8 α -positive cells in thyroid cancer samples. Therefore, our results suggest that tumor immunity plays a protective role against cancer progression in *Thrb^{PV/PV}* mice, which is regulated by testosterone.

Testosterone regulation of thyroid cancer progression is likely complex, but based on our findings and published data, we postulate that testosterone promotes thyroid cancer progression through suppressing immune surveillance against cancer and by reducing tumor suppressor gene (*Glipr1* and *Sfrp1*) expression. The suppressed *Glipr1* expression could further reduce the immune response and tumor immune cell infiltration as

we observed GLIPR1 knockdown *in vitro* resulted in decreased Ccl5 secretion, a known chemokine with a role in activation of immune cells (13,18,21). These events result in reduced control of cancer growth, leading to cancer progression.

Although FTC is the second most common type of human thyroid cancer, it is particularly aggressive and is associated with a higher mortality due to uncontrolled locally advanced and metastatic disease, providing us with a rationale for using the *Thrb^{PV/PV}* transgenic mouse model to study the effects of sex hormones on thyroid cancer initiation and progression. Furthermore, TR β inactivation is frequently seen in human thyroid cancer samples, making it a relevant model to use for our studies (29). For these reasons, we believe our findings are relevant to human thyroid cancer.

In summary, our study shows that testosterone plays an important role in the progression of FTC. In a FTC mouse model, female sex hormones increased cancer initiation consistent with the higher rates of human FTC observed in women. On the other hand, male sex hormone (testosterone) promotes FTC progression in mice consistent with the more aggressive disease observed for human FTC in men. The effect of testosterone on cancer progression is mediated through regulating the expression of tumor suppressor and immune-regulatory genes and modulating tumor immune response.

Supplementary material

Supplementary Tables S1–S5 and Figures S1–S5 can be found at <http://carcin.oxfordjournals.org/>

Funding

Center for Cancer Research, National Cancer Institute, National Institutes of Health. Grant number: ZIA BC011275 05.

Acknowledgements

We are grateful to Dr Myriem Boufraquech, Dr Sudheer Gara of National Cancer Institute/National Institutes of Health (USA), Dr Xiaolin Wu, Dr Ling Su (Frederick National Laboratory for Cancer Research, Frederick, MD, USA) and Ms. Elena Kuznetsova for technical help.

Conflict of Interest Statement: None declared.

References

1. Fajkovic, H. et al. (2011) Impact of gender on bladder cancer incidence, staging, and prognosis. *World J. Urol.*, 29, 457–463.
2. Rahbari, R. et al. (2010) Thyroid cancer gender disparity. *Future Oncol.*, 6, 1771–1779.
3. Mulligan, C.R. et al. (2006) Unlimited access to care: effect on racial disparity and prognostic factors in lung cancer. *Cancer Epidemiol. Biomarkers Prev.*, 15, 25–31.
4. Davies, L. et al. (2006) Increasing incidence of thyroid cancer in the United States, 1973–2002. *JAMA*, 295, 2164–2167.
5. Nilubol, N. et al. (2013) Multivariate analysis of the relationship between male sex, disease-specific survival, and features of tumor aggressiveness in thyroid cancer of follicular cell origin. *Thyroid*, 23, 695–702.
6. Aschebrook-Kilfoy, B. et al. (2011) Diabetes and thyroid cancer risk in the National Institutes of Health-AARP Diet and Health Study. *Thyroid*, 21, 957–963.
7. Shih, S.R. et al. (2012) Diabetes and thyroid cancer risk: literature review. *Exp. Diabetes Res.*, 2012, 578285.
8. Kitahara, C.M. et al. (2011) Obesity and thyroid cancer risk among U.S. men and women: a pooled analysis of five prospective studies. *Cancer Epidemiol. Biomarkers Prev.*, 20, 464–472.

9. Ruggieri, A. et al. (2010) Cellular and molecular mechanisms involved in hepatocellular carcinoma gender disparity. *Int. J. Cancer*, 127, 499–504.
10. Nakagawa, H. et al. (2009) Serum IL-6 levels and the risk for hepatocarcinogenesis in chronic hepatitis C patients: an analysis based on gender differences. *Int. J. Cancer*, 125, 2264–2269.
11. Naugler, W.E. et al. (2007) Gender disparity in liver cancer due to sex differences in MyD88-dependent IL-6 production. *Science*, 317, 121–124.
12. Suzuki, H. et al. (2002) Mice with a mutation in the thyroid hormone receptor beta gene spontaneously develop thyroid carcinoma: a mouse model of thyroid carcinogenesis. *Thyroid*, 12, 963–969.
13. Lapteva, N. et al. (2010) CCL5 as an adjuvant for cancer immunotherapy. *Expert Opin. Biol. Ther.*, 10, 725–733.
14. Kaneshige, M. et al. (2000) Mice with a targeted mutation in the thyroid hormone beta receptor gene exhibit impaired growth and resistance to thyroid hormone. *Proc. Natl Acad. Sci. USA*, 97, 13209–13214.
15. Xu, X. et al. (2007) Quantitative measurement of endogenous estrogens and estrogen metabolites in human serum by liquid chromatography-tandem mass spectrometry. *Anal. Chem.*, 79, 7813–7821.
16. Klug, F. et al. (2013) Low-dose irradiation programs macrophage differentiation to an iNOS⁺/M1 phenotype that orchestrates effective T cell immunotherapy. *Cancer Cell*, 24, 589–602.
17. Li, L. et al. (2011) GLIPR1 suppresses prostate cancer development through targeted oncoprotein destruction. *Cancer Res.*, 71, 7694–7704.
18. Satoh, T. et al. (2003) Adenoviral vector-mediated mRTVP-1 gene therapy for prostate cancer. *Hum. Gene Ther.*, 14, 91–101.
19. Ren, C. et al. (2002) mRTVP-1, a novel p53 target gene with proapoptotic activities. *Mol. Cell. Biol.*, 22, 3345–3357.
20. Li, L. et al. (2008) Glioma pathogenesis-related protein 1 exerts tumor suppressor activities through proapoptotic reactive oxygen species-c-Jun-NH2 kinase signaling. *Cancer Res.*, 68, 434–443.
21. Sonpavde, G. et al. (2011) GLIPR1 tumor suppressor gene expressed by adenoviral vector as neoadjuvant intraprostatic injection for localized intermediate or high-risk prostate cancer preceding radical prostatectomy. *Clin. Cancer Res.*, 17, 7174–7182.
22. Li, L. et al. (2013) Glioma pathogenesis-related protein 1 induces prostate cancer cell death through Hsc70-mediated suppression of AURKA and TPX2. *Mol. Oncol.*, 7, 484–496.
23. Karantanos, T. et al. (2014) Systemic GLIPR1-ΔTM protein as a novel therapeutic approach for prostate cancer. *Int. J. Cancer*, 134, 2003–2013.
24. Chow, M.T. et al. (2012) Inflammation and immune surveillance in cancer. *Semin. Cancer Biol.*, 22, 23–32.
25. Guarino, V. et al. (2010) Thyroid cancer and inflammation. *Mol. Cell. Endocrinol.*, 321, 94–102.
26. Okayasu, I. et al. (1995) Association of chronic lymphocytic thyroiditis and thyroid papillary carcinoma. A study of surgical cases among Japanese, and white and African Americans. *Cancer*, 76, 2312–2318.
27. Kebebew, E. et al. (2001) Coexisting chronic lymphocytic thyroiditis and papillary thyroid cancer revisited. *World J. Surg.*, 25, 632–637.
28. Fiumara, A. et al. (1997) In situ evidence of neoplastic cell phagocytosis by macrophages in papillary thyroid cancer. *J. Clin. Endocrinol. Metab.*, 82, 1615–1620.
29. Kim, W.G. et al. (2013) Reactivation of the silenced thyroid hormone receptor β gene expression delays thyroid tumor progression. *Endocrinology*, 154, 25–35.